







Water Resources Research®



RESEARCH ARTICLE

10.1029/2022WR034023

The Impact of Soil Tension on Isotope Fractionation, Transport, and Interpretations of the Root Water Uptake Origin

Tiantian Zhou¹ , Jiří Šimůnek¹ , Paolo Nasta² , Giuseppe Brunetti³ , Marcel Gaj⁴ , Christoph Neukum⁵, and Vincent Post⁶ 

¹Department of Environmental Sciences, University of California Riverside, Riverside, CA, USA, ²Department of Agricultural Sciences, AFBE Division, University of Naples Federico II, Napoli, Italy, ³Department of Civil Engineering, University of Calabria, Rende, Italy, ⁴Department of Hydrology, State Agency for Nature, Environment and Consumer Protection, Minden, Germany, ⁵Federal Institute for Geosciences and Natural Resources (BGR), Hannover, Germany, ⁶Edinsi Groundwater, Nederhorst den Berg, The Netherlands

Key Points:

- While factors in the Craig-Gordon equation dominate evaporation fractionation, soil tension effects deplete isotopic composition of surface soil water
- Root water uptake origin interpreted by considering tension effects is between no fractionation and Craig-Gordon fractionation scenarios
- Using the Bayesian isotope mixing model or the virtual tracer experiment is more demanding than water balance or particle tracking methods

Supporting Information:

Supporting Information may be found in the online version of this article.

Correspondence to:

T. Zhou and V. Post,
tzhou035@ucr.edu;
vincent@edinsi.nl

Citation:

Zhou, T., Šimůnek, J., Nasta, P., Brunetti, G., Gaj, M., Neukum, C., & Post, V. (2023). The impact of soil tension on isotope fractionation, transport, and interpretations of the root water uptake origin. *Water Resources Research*, 59, e2022WR034023. <https://doi.org/10.1029/2022WR034023>

Received 18 NOV 2022

Accepted 3 AUG 2023

Abstract The new isotope module in HYDRUS-1D can be used to infer the origin of root water uptake (RWU), a suitable dynamic indicator for agriculture and forest water management. However, evidence shows that the equilibrium fractionation between liquid water and water vapor within the soil is affected not only by soil temperature but also by soil tension. How soil tension affects isotope transport modeling and interpretations of the RWU origin is still unknown. In this study, we evaluated three fractionation scenarios on model performance for a field data set from Langeoog Island: (a) no fractionation (Non_Frac), (b) the soil temperature control on equilibrium fractionation as described by the standard Craig-Gordon equation (CG_Frac), and (c) CG_Frac plus the soil tension control on equilibrium fractionation (CGT_Frac). The model simulations showed that CGT_Frac led to more depleted isotopic compositions of surface soil water than CG_Frac. The vertical origin of RWU was estimated using the water balance (WB) calculations and the Bayesian mixing model (SIAR). While the former directly used water flow outputs, the latter used as input simulated isotopic compositions (using different fractionation scenarios) of RWU and soil water. Both methods provided similar variation trends with time and depth in different soil layers' contributions to RWU. The contributions of all soil layers interpreted by the CGT_Frac scenario were always between Non_Frac and CG_Frac. The temporal origin of RWU was deduced from particle tracking (PT, releasing one hypothetical particle for individual precipitation event and tracking its movement based on the water balance between particles) and a virtual tracer experiment (VTE, assigning a known isotope composition to individual precipitation event and tracking its movement based on the cumulative isotope flux). Both methods revealed similar variation trends with time in drainage and root zone (RZ) travel times. The interpreted drainage and RZ travel times were generally ranked as Non_Frac > CGT_Frac > CG_Frac. Overall, the factors considered in the standard CG equation dominated isotope fractionation, transport, and interpretations of the RWU origin. Isotope transport-based methods (SIAR, VTE) were more computationally demanding than water flow-based methods (WB, PT).

1. Introduction

Equilibrium and kinetic fractionation processes occur between soil water vapor and liquid water or within soil water vapors and induce enrichment of stable isotopes of hydrogen (²H) and oxygen (¹⁸O) in the remaining soil water during evaporation. Kinetic fractionation is influenced by transport resistances from the evaporating surface to the atmosphere and isotope diffusivities. Equilibrium fractionation is usually determined as a function of soil temperature (Majoube, 1971). However, recent research shows that soil tension can affect equilibrium fractionation by influencing interactions between water films on soil particle surfaces and water vapor (Bowers et al., 2020; Lin et al., 2018; Lin & Horita, 2016; Orłowski & Breuer, 2020). Soil tension represents the free energy required to remove water from the soil matrix and induces the water vapor pressure deficit within the soil. At very high soil tensions (i.e., dry conditions), the surface of soil particles preferentially attracts lighter isotopes due to limited surface free energy, and soil water vapor diffusion from the soil bottom toward the atmosphere increases. As a result, tightly bound soil water (i.e., slow mobile water subject to capillary-driven flow) is thus depleted of heavy isotope species, which induces the enrichment in isotopic signatures of surface soil water vapor (Gaj & McDonnell, 2019).

© 2023. The Authors.

This is an open access article under the terms of the [Creative Commons Attribution-NonCommercial-NoDerivs License](https://creativecommons.org/licenses/by-nc-nd/4.0/), which permits use and distribution in any medium, provided the original work is properly cited, the use is non-commercial and no modifications or adaptations are made.

Not considering this factor in the modeling analysis may have implications for interpreting the origin of water fluxes in the soil-plant-atmosphere continuum. Considerable attention has been paid to the vertical and temporal origin of root water uptake (RWU) because this information can guide when and how much to irrigate, maximize RWU, and reduce deep percolation, thus improving agricultural water use efficiency.

The vertical origin of root water uptake (RWU) across the soil profile has been (a) determined graphically by comparing the isotopic characteristics of xylem water and soil water at different depths in the dual-isotope plots, (b) calculated by linear mixing models, or (c) estimated using statistical models such as the IsoSource and Bayesian mixing models (SIAR, MixSIR, and MixSIAR). Multiple Bayesian models (i.e., SIAR, MixSIR, and MixSIAR) were compared by Wang et al. (2019), who reported better performance of SIAR and MixSIAR in identifying water sources. Compared with the IsoSource model, the Bayesian mixing models can accurately estimate water sources for RWU while simultaneously considering their uncertainty (e.g., Zhang et al., 2022).

Compared with the vertical origin, research on the temporal origin of RWU (especially numerical modeling studies) has been limited to a few studies (Allen et al., 2019; Brinkmann et al., 2018; Luo et al., 2023; Miguez-Macho & Fan, 2021; Zhou et al., 2022). An important premise for inferring the temporal origin of RWU is an accurate estimate of travel times (TT) of irrigation/precipitation water to different depths in the soil profile (e.g., to the bottom of the soil profile as drainage or the root zone (RZ) as RWU, etc.). As summarized in Sprenger et al. (2019), the three common methods to estimate travel times include (a) time-invariant TT distributions, (b) StorAge Selection (SAS) functions, and (c) flux tracking or particle tracking (PT) implemented in physically based hydrological models. The first two methods require the optimization of isotope transport parameters in lumped models (Asadollahi et al., 2020; Benettin et al., 2015; Harman, 2015; Kim & Harman, 2022; Maloszewski et al., 2006; Pangle et al., 2017; Rinaldo et al., 2015; Stumpp & Maloszewski, 2010; Tetzlaff et al., 2014, 2018; Timbe et al., 2014). However, these lumped models oversimplify the isotope transport mechanisms (Sprenger et al., 2016, 2019).

By contrast, physically based numerical models (e.g., the isotope-enabled module in HYDRUS-1D) have the potential to continuously assess the spatio-temporal origin of RWU, by solving water flow and isotope transport using the Richards and the advection-dispersion equations, respectively (Stumpp et al., 2012; Zhou et al., 2021, 2022). However, reliable model simulations are obtained only when the model setup accurately describes water flow and isotope transport (Finkenbiner et al., 2022). Brinkmann et al. (2018) employed a flux tracking approach (virtual tracer experiment) using the isotope-enabled module in HYDRUS-1D (neglecting evaporation fractionation, Stumpp et al., 2012) to derive the residence time distribution of precipitation in the soil and the temporal origin of RWU in a temperate forest. They found that 50% of water consumed by trees throughout the year came from precipitation during the growing season (May–October), while 40% of it originated from precipitation in the preceding winter (November–April) (Brinkmann et al., 2018).

A recent module implemented in HYDRUS-1D considers evaporation fractionation in isotope transport modeling (Zhou et al., 2021), in which equilibrium fractionation is controlled only by soil temperature. Post et al. (2022) found that considering evaporation fractionation in the code of Zhou et al. (2021) could significantly improve the isotope transport modeling on Langeoog Island. Zhou et al. (2022) used PT in HYDRUS-1D and found that considering fractionation in the code of Zhou et al. (2021) resulted in longer residence times of precipitation in soil and older water ages of RWU for winter rye in a lysimeter. However, isotope transport modeling has often ignored various factors influencing evaporation fractionation (e.g., soil tension). Although this does not affect water flow, it affects the isotope mass balance and simulated isotopic signals. This may also introduce the risk of erroneously interpreting the origin of RWU when using isotope transport-based methods. Nevertheless, little research has been carried out to compare the water flow-based (i.e., water balance and PT, which may act as a benchmark) and isotope transport-based (i.e., SIAR, virtual tracer experiment) methods in interpreting the origin of RWU for different evaporation fractionation scenarios.

Therefore, we pose the following three scientific questions.

1. To what extent does the consideration of the soil tension control on equilibrium evaporation fractionation affect the performance and isotope mass balance of the isotope transport model?
2. How will different modeling results (based on different fractionation scenarios) affect the interpretation of the spatio-temporal origin of RWU?
3. Is it better to use water-flow-based (water balance, PT) or isotope-transport-based (SIAR, virtual tracer experiment) methods to determine the spatio-temporal origin of RWU?

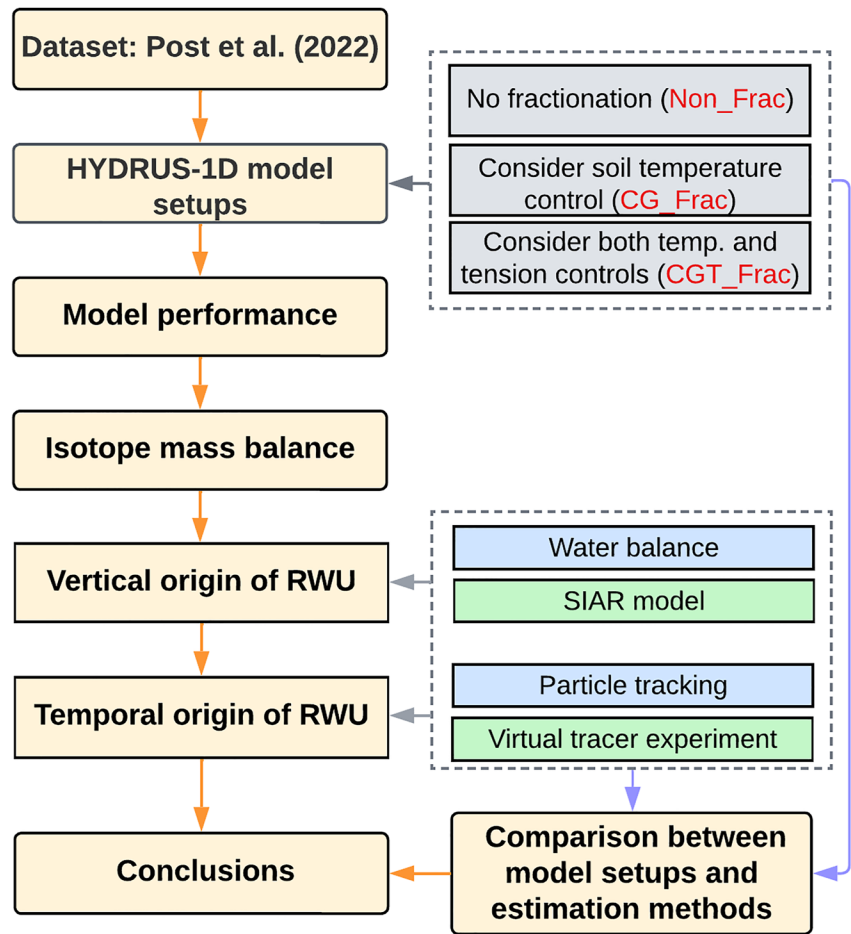


Figure 1. Schematic outline of methods used. Model setup considered three fractionation scenarios (gray boxes), including Non_Frac, CG_Frac, and CGT_Frac indicating no fractionation, fractionation described by the standard Craig-Gordon equation with only soil temperature control on equilibrium fractionation, and fractionation according to the modified Craig-Gordon equation with both soil temperature and tension controls on equilibrium fractionation, respectively. The origin of root water uptake is based on either water-flow-based methods (blue boxes) or isotope-transport-based methods (green boxes).

To answer these three scientific questions, we used isotope data collected across a 450-cm-thick soil profile beneath grassland on Langeoog Island (Post et al., 2022) in combination with modified HYDRUS-1D (Zhou et al., 2021) to study the influence of soil tension effects on the isotope fractionation and transport modeling, and to evaluate how different model setups and estimation methods affect the interpretation of isotopes signals in determining the spatio-temporal origin of RWU (Figure 1). Since a one-dimensional model is used in this study, any references to spatial distributions refer to vertical/depth distributions.

2. Materials and Methods

2.1. Study Area and Data Collection

Langeoog is a sandy barrier island off the coast of northern Germany. The annual precipitation rate on Langeoog Island is 777 mm (Houben et al., 2014). The freshwater groundwater lens is the only water source on this island that helps balance water levels between island groundwater and seawater and prevents seawater intrusion. However, this dynamic balance is fragile due to years of extensive groundwater pumping over the years resulting from intensive tourism and seawater erosion of the island (Post et al., 2022).

Many natural or artificial dunes have been created to protect the coast from erosion (Post & Houben, 2017). Over several years, these dunes have shifted from an almost unvegetated type to a vegetated kind, covered with

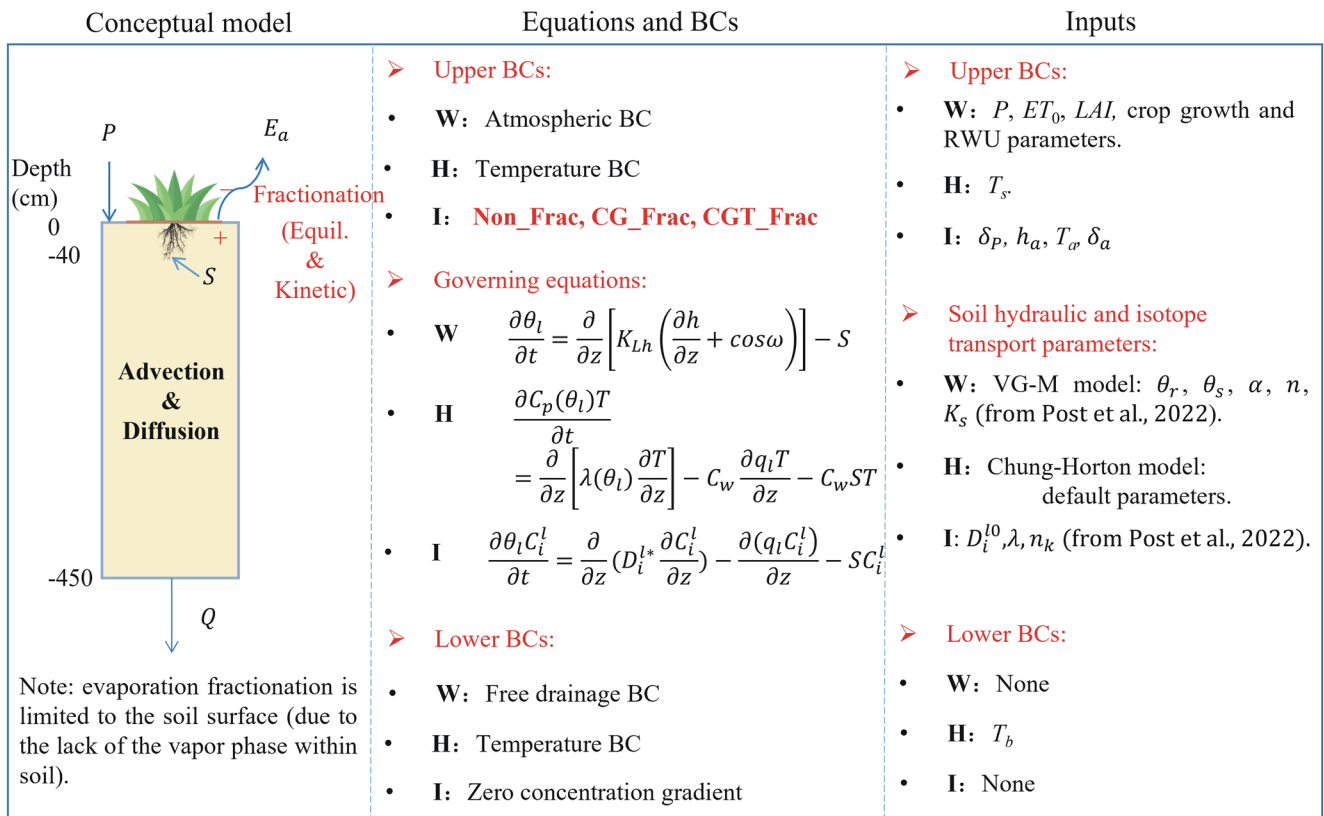


Figure 2. HYDRUS-1D model setup. W, H, and I represent water flow, heat transport, and isotope transport, respectively. Boundary condition (BC) denotes BC. Note that the description of the variables in this figure is shown in Table S1 in Supporting Information S1.

mosses, grass, and low shrubs (Post et al., 2022). This vegetation change may bring about changes in groundwater recharge processes due to increased RWU and transpiration. Many studies have been conducted on temporal variations of groundwater recharge in this dune area (Houben et al., 2014; Post et al., 2022). However, characterizing travel times of precipitation to RWU and groundwater recharge is still lacking, while enhancing this understanding is critical for the sustainable development of groundwater resources on this island.

Additionally, the dune sands are very dry due to evaporation and RWU, and its surface soil water is enriched with heavy isotopes due to evaporation fractionation (Post et al., 2022). These conditions make it a good site for studying the impacts of soil tension control on evaporation fractionation. The vegetated dune (Site LB01 in Post et al. (2022), covered by grasses) was selected in this study to analyze the origin of its vegetation RWU.

The experiment was carried out between July 2012 and June 2019 in a 450-cm-thick soil profile. The meteorological data, including daily precipitation P , air humidity (h_a), and mean/maximum/minimum air temperature (T_a), were measured at daily time resolution. Precipitation samples for isotopic compositions were collected fortnightly or monthly. Soil samples were collected on 25 June 2019 (10–425 cm below the soil surface, about every 5 or 10 cm) to measure grain size, soil water contents, and soil water isotopic compositions. Soil hydraulic properties were measured on soil cores collected at the nearby site (Figure 1 of Post et al., 2022) during an earlier project in 2014 using the evaporation method carried out on the HYPROP semi-automatic device (METER Group, Munich, Germany) (Lipovetsky et al., 2020). The temporal distributions of relevant weather and vegetation growth variables are shown in Figures S1 and S2 in Supporting Information S1. More details about the study area and data collection methods can be found in (Post et al., 2022).

2.2. HYDRUS-1D Model Setup

Water flow and isotope transport in the unsaturated zone were simulated using a modified version of the HYDRUS-1D code that considers isotope evaporation fractionation (Zhou et al., 2021). Figure 2 shows a

summary of the model setup. The simulation period is 2536 days long (corresponding to about 7 years), from 17 July 2012, to 25 June 2019. The 450-cm-thick soil profile is uniform with a single set of soil hydraulic (θ_p , θ_s , α , n , K_s) and isotope transport (D_i^{l0} , λ , n_k) parameters (Table S1 and Figure S8 in Supporting Information S1).

The actual RWU rate of grass, S within the RZ depends on the rooting depth and the root density distribution (Figure S1 in Supporting Information S1). It is obtained from potential RWU and the stress response function depending on the pressure head (Feddes et al., 1978).

The upper boundary condition (BC) is set to the potential water flux across the soil surface (i.e., the difference between daily values of potential evapotranspiration, ET_p , and precipitation, P), while the lower BC is set to free drainage (a zero pressure head gradient). Temperature BC is used at upper and lower boundaries for heat transport. Daily isotope concentrations, δ_p , are assigned to their corresponding precipitation events to get the concentration flux for the upper BC, while a zero concentration gradient (i.e., free drainage) is set as the lower BC. The initial soil water content ($0.046 \text{ cm}^3/\text{cm}^3$), temperature (20°C) and isotopic composition (-110 ‰ for ^2H and -10 ‰ for ^{18}O) are used throughout the soil profile. Post et al. (2022) provide more details about the model setups.

In our analysis, three fractionation scenarios have been considered, including (a) no evaporation fractionation (the Non_Frac scenario), (b) evaporation fractionation described by the Craig-Gordon equation, which considers only the soil temperature control on equilibrium fractionation (the CG_Frac scenario), and (c) evaporation fractionation according to the modified Craig-Gordon equation, which considers both the soil tension and soil temperature controls on equilibrium fractionation (the CGT_Frac scenario).

2.2.1. Craig-Gordon Equation

Evaporation fractionation between the soil water and the free atmosphere includes both equilibrium and kinetic fractionation processes (Craig, 1961). Craig and Gordon (1965) calculated the isotope evaporation flux at the soil surface based on these two types of fractionations.

When the isotope concentration is expressed in kg m^{-3} (Eq. 1 in Zhou et al., 2021), the isotope evaporation flux E_i ($\text{kg m}^{-2} \text{ s}^{-1}$) is:

$$E_i = E_i^{\text{out}} - E_i^{\text{in}} = \frac{E_a M_i}{\alpha_i^k M_w} \frac{(RH_s \cdot \alpha_{v/w} \cdot R_L - RH_a' \cdot R_a)}{RH_s - RH_a'} \quad (1)$$

The isotope ratio of the evaporation flux $R_E [-]$ is expressed as:

$$R_E = E_i/E_a = [RH_s \cdot \alpha_{v/w} \cdot R_L - RH_a' \cdot R_a] / [(RH_s - RH_a') \cdot \alpha_i^k] \cdot \frac{M_i}{M_w} \quad (2)$$

where E_a (m/s) is the actual evaporation flux, M_i and M_w (kg/mol) are the molar masses of heavy water and ordinary water, respectively, $RH_s [-]$ is the relative humidity of the surface soil air phase, $RH_a' [-]$ is the normalized air relative humidity, $R_L [-]$ is the isotope ratio of the remaining surface liquid water, $R_a [-]$ is the isotope ratio of the atmospheric water vapor, and $\alpha_{v/w}$ and $\alpha_i^k [-]$ are the equilibrium and kinetic fractionation factors, respectively. We only show the calculation of $\alpha_{v/w}$ in the main manuscript. Calculations of other variables are shown in Text S1 in Supporting Information S1.

2.2.2. Temperature Control on Equilibrium Fractionation

Majoube (1971) computed the equilibrium fractionation factor $\alpha_{v/w}$ as a function of temperature T (K):

$$\alpha_{v/w}(^2\text{H}/^1\text{H})_{\text{majoube}} = \exp\left(-52.612 \cdot 10^{-3} + \frac{76.248}{T} - \frac{24.844 \cdot 10^3}{T}\right) \quad (3)$$

$$\alpha_{v/w}(^{18}\text{O}/^{16}\text{O})_{\text{majoube}} = \exp\left(2.0667 \cdot 10^{-3} + \frac{0.4156}{T} - \frac{1.137 \cdot 10^3}{T^2}\right) \quad (4)$$

2.2.3. Tension Control on Equilibrium Fractionation

The equilibrium fractionation factor is affected not only by temperature but also by soil tension when it is above 1,260 hPa (about 1,284 cm) under dry conditions (Gaj & McDonnell, 2019). The empirical equations presented by Gaj and McDonnell (2019) express the equilibrium fractionation factor $\alpha_{v/w}$ as the contribution of $\alpha_{v/w_{\text{majoube}}}$

and the effect of soil tension, $\text{abs}(h)$ (absolute values of soil matric potential h , cm), which is independent of soil texture:

$$\alpha_{v/w}(^2H/^1H) = \alpha_{v/w}(^2H/^1H)_{\text{majoube}} + 0.01498 \log_{10}(\text{abs}(h)) \quad (5)$$

$$\alpha_{v/w}(^{18}O/^{16}O) = \alpha_{v/w}(^{18}O/^{16}O)_{\text{majoube}} + 0.00607 \log_{10}(\text{abs}(h)) \quad (6)$$

The new isotope transport module used in this study is almost the same as in Zhou et al. (2021). Specifically, both modules require the input of the atmospheric water vapor's relative humidity, temperature, and isotopic composition (Equation 1). The only difference is that the soil tension control on the equilibrium fractionation factor $\alpha_{v/w}$ can be optionally considered in the model. Note that the equilibrium fractionation factor $\alpha_{v/w}$ is 1 in the Non_Frac scenario (Stump et al., 2012), smaller than 1 in the CG_Frac (Equations 3 and 4), but may be greater or smaller than 1 in the CGT_Frac because of the tension control (Equations 5 and 6).

2.3. Interpreting the Origin of Root Water Uptake

The results of the three modeling scenarios were used to interpret the vertical and temporal origin of RWU using both water flow- (water balance, PT) and isotope transport-based (SIAR, virtual tracer experiment) methods. Note that all calculations were conducted on a daily interval.

2.3.1. Vertical Origin of Root Water Uptake

Soil water at different depths of the RZ represents the source of RWU. The 40-cm-thick RZ was divided into four sub-layers (0–10, 10–20, 20–30, and 30–40 cm), considered separate water sources (Layer 1, Layer 2, Layer 3, Layer 4, respectively). Capillary rise from groundwater was not considered because of a relatively shallow maximum rooting depth (40 cm) and deep water table (below 450 cm) in this study area. The contributions of different soil layers to RWU were assessed using two methods.

The first method is the water balance calculation, in which RWU from different soil layers was directly retrieved using information printed by HYDRUS-1D. The second method is the SIAR Bayesian isotope mixing model (Parnell et al., 2010) implemented in the R package. SIAR is widely used in estimating the contributions of different source tracers to a mixture tracer. In this model, each source tracer value and its standard error (because of measurement errors, discrimination factors, etc.) are assumed to follow normal distributions. The mixture tracer value is the sum of different source tracer values multiplied by their corresponding proportional contributions and the residual error. More details can be found in Cao et al. (2022) and Stock et al. (2018).

In this study, different fractionation scenarios were first simulated using the HYDRUS-1D model to obtain isotopic compositions of RWU (root isotope uptake divided by RWU) and isotopic compositions of soil water at different depths. Simulated δ^2H and $\delta^{18}O$ in RWU and soil water in different layers and corresponding standard errors were then used as the mixture and source tracer values in the SIAR model. The discrimination values were set to zero for both δ^2H and $\delta^{18}O$ because there is usually no isotope fractionation during RWU (Dawson & Ehleringer, 1991).

The Mann-Kendall trend test was used to determine whether there is a trend (indicated by τ values; positive and negative τ values indicate increasing and decreasing trends, respectively) in the time series of contributions of different water sources to RWU obtained by both methods. The null hypothesis is that the data has no trend ($\tau = 0$). When the p -value of the test is below a certain significance level ($p < 0.01$ was used in this study), it can be concluded that there is a statistically significant trend in the investigated time series.

2.3.2. Temporal Origin of Root Water Uptake

2.3.2.1. Particle Tracking (PT)

The PT algorithm (Figure S3 and Text S2 in Supporting Information S1) requires two input parameters: w_{Stand} and w_{Prec} (Zhou et al., 2021, 2022; Šimůnek, 1991). In this study, the input parameters w_{Stand} and w_{Prec} were set to 10 cm and a negative value, respectively. The former represents the water storage that separates adjacent particles in the soil profile at the beginning of the simulation. The latter negative value causes the program to release one particle for each precipitation event so that one can track the movement of each precipitation event separately. The PT algorithm then calculates particle positions based on water mass balance calculations between

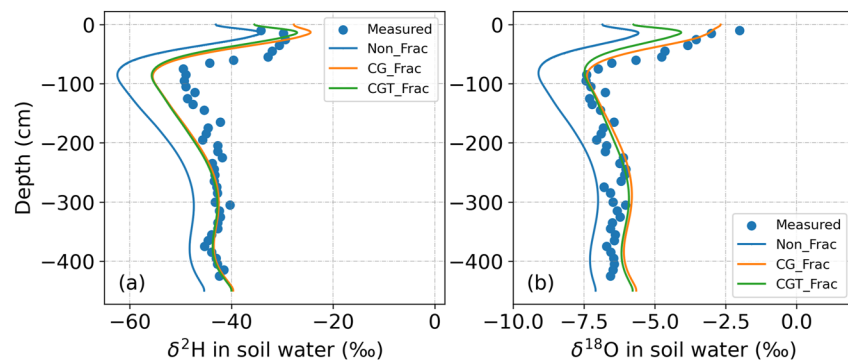


Figure 3. Measured (blue circles) and simulated (a) $\delta^2\text{H}$ and (b) $\delta^{18}\text{O}$ profiles at the end of the simulation (25 June 2019) for three fractionation scenarios (Non_Frac, CG_Frac, and CGT_Frac).

two neighboring particles (and the soil surface) during a specific time interval. Based on particle positions at different times, one can deduce the residence times of each precipitation event for various soil depths. The difference between the times when a particle enters and leaves the soil profile (or the RZ) is defined as drainage (or RZ) travel time. The PT module also evaluates the contribution of each particle to RWU at different times, which can be used to infer the temporal origin of RWU.

2.4. Virtual Tracer Experiment (VTE)

The virtual tracer experiment (VTE) method (Figure S4 in Supporting Information S1) was used to interpret drainage and RZ travel times for different fractionation scenarios based on repeated simulations of isotope transport using HYDRUS-1D (Nasta et al., 2021). HYDRUS-1D is run n times (where n equals the number of precipitation events), assuming the initially isotope-free soil profile, assigning a known isotope composition to the i th precipitation event, and keeping all remaining rainfall events isotope-free. This technique helps trace isotope composition across the soil profile from every individual rainfall event. The arrival (or exit) time is calculated when the cumulative isotope flux at the soil profile bottom reaches 50% of its final value. The travel time is calculated as a difference between precipitation entry times and arrivals.

3. Results

To assess the possible impact of the soil tension control on equilibrium fractionation under various soil temperature and tension conditions, we carried out a preliminary sensitivity analysis of $\alpha_{v/w}$ to soil temperature (from 0 to 45°C, i.e., from 273.15 to 318.15 K) and tension (1,284, 2,500, 5,000, 10,000 cm) (Text S3 in Supporting Information S1). The results show that the contribution of the soil tension control on $\alpha_{v/w}$ (lower than 6.5% and 2.5% for ^2H and ^{18}O , respectively) is always smaller than that of soil temperature control. Overall, the soil tension control has a higher impact on $\alpha_{v/w}$ of ^2H than ^{18}O . However, whether this small contribution results in a considerable difference in isotopic compositions, isotope mass balance components, and the interpretations of RWU origin needs to be further explored.

3.1. Model Performance and Isotope Mass Balance

The model performance for the final isotopic composition profiles of each modeling scenario is shown in Figure 3, and the corresponding root mean square errors (RMSE) are reported in Table 1. The model performance of the CG_Frac and CGT_Frac scenarios were quite similar, although very different from the Non_Frac scenario. The Non_Frac scenario produced lower isotopic compositions of surface soil water than the CG_Frac and CGT_Frac scenarios. On the other hand, the scenario that considered the soil tension control (CGT_Frac) predicted the isotopic composition of surface soil water to be more depleted (by -7.8‰ for $\delta^2\text{H}$ and -3.1‰ for $\delta^{18}\text{O}$) in this example than the CG_Frac scenario.

The impact of isotope fractionation controlled by the standard Craig-Gordon (CG) equation and soil tension on the model simulations was evaluated as a percentage of a contribution to the RMSE. As can be seen in

Table 1
Root Mean Square Error (RMSE) Values ($RMSE_{\delta^2H}$, $RMSE_{\delta^{18}O}$, and $RMSE_{avg}$ Refer to RMSEs for the δ^2H , $\delta^{18}O$, and Average, Respectively) for Different Fractionation Scenarios (Non_Frac, CG_Frac, and CGT_Frac)

RMSE (%)	Non_Frac	CG_Frac	CGT_Frac	CG_Frac relative to Non_Frac	CGT_Frac relative to CG_Frac	CGT_Frac relative to Non_Frac	Contribution of the standard CG equation (%)	Contribution of tension control (%)
$RMSE_{\delta^2H}$	10.06	5.06	5.42	-5.00	0.35	-4.64	93	7
$RMSE_{\delta^{18}O}$	1.66	0.56	0.79	-1.09	0.23	-0.87	83	17
$RMSE_{avg}$	5.86	2.81	3.10	-3.05	0.29	-2.75	91	9

Table 1, considering the standard CG equation (CG_Frac) almost halved RMSEs. Adding soil tension controls (CGT_Frac) also halved RMSEs, thus obtaining similar performance. In other words, adding tension control does not provide substantial benefits and even slightly increased RMSEs in this example. The impact of considering the CG model and tension controls on $RMSE_{avg}$ was 91% and 9%, respectively. The factors considered in the standard CG equations led the model performance.

Various isotope mass balance components were also evaluated to understand the reasons behind differences in model performance and subsequent practical applications of different fractionation scenarios (Text S4 and Table S2 in Supporting Information S1). Overall, the isotope mass balance components in the CGT_Frac were almost always between the Non_Frac and CG_Frac. The impact of considering the CG model on the isotope mass balance was 66% for 2H and 57% for ^{18}O , while the impact of considering the soil tension control was 34% for 2H and 43% for ^{18}O . The factors considered in the standard CG equation dominated the isotope mass balance.

3.2. Vertical Origin of Root Water Uptake

The dynamics of contributions of the four soil layers to RWU obtained using the water balance method and the SIAR model are shown in Figures 4 and 5 and Table 2 (note that their sum is one). Since the same set of soil hydraulic parameters was used in all fractionation scenarios, the results of the vertical origin of RWU remained the same when using the water balance method.

According to the Mann-Kendall trend tests (Text S5 in Supporting Information S1), the contribution of the 0–10 cm soil layer (i.e., Layer 1) showed a decreasing trend (characterized by negative τ values) with the largest fluctuations. The contributions of the other soil layers showed increasing trends (suggested by positive τ values) and were relatively stable. This is because the functioning of the top layer (0–10 cm) is different from the other layers as it is affected by evaporation fractionation during the dry season and mixing during precipitation (Barnes & Turner, 1998). The deeper soil layers gradually became more important water sources, probably due to the lack of rainfall (Figure S2 in Supporting Information S1), which increased the root water stress in the surface soil and promoted uptake from deeper layers. The contributions decreased from Layer 1 to 4 because the root density decreased as soil depths increased (Figure S1 in Supporting Information S1).

In general, considering fractionation (CG_Frac, CGT_Frac) interpreted a decrease in the simulated contribution of Layer 1 and an increase in contributions for the other soil layers (Table 2). Overall, the contributions in

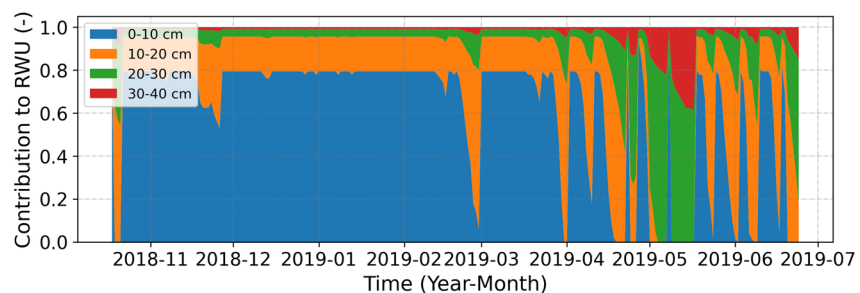


Figure 4. The contributions of different soil layers ((a) 0–10 cm, (b) 10–20 cm, (c) 20–30 cm, and (d) 30–40 cm) to root water uptake for the last 250 days of the simulation (2018/10/18–2019/06/25) calculated using the water balance method.

the CGT_Frac scenario were always between Non_Frac and CG_Frac for all soil layers. Table 2 (the last two columns) shows that the factors considered in the standard CG equation played a dominant role in interpreting the contributions of all soil layers to RWU.

3.3. Temporal Origin of Root Water Uptake

3.3.1. Particle Tracking

Since the same set of parameters was used in all fractionation scenarios, the temporal origin of RWU remained the same when using the PT method. The residence time distribution of precipitation in soil water and the temporal origin of RWU showed seven cycles in the entire simulation period (Figures 6a and 6b). Only the last 250 days (2018/10/18–2019/06/25) of the relative frequency distributions of drainage and RZ travel times (Figures 6c and 6d) are displayed to be consistent with the display of the results of the isotope transport-based methods. During this period, the drainage travel times decreased with time (Figure 6a). RWU in each month except April and May of 2019, mainly (more than 60%) originated from the current month's precipitation (Figure 6b). The corresponding mean drainage and RZ travel times were about 230.96 and 12.64 days, respectively (Figures 6c and 6d, Table 3).

3.3.2. Virtual Tracer Experiment

Figures 7 and 8 show the dynamics of drainage and RZ travel times interpreted by different fractionation scenarios using the virtual tracer experiment. The drainage travel times generally decreased with time (Figure 7d) because discharge increased overall with time (Figure 7c). There were always apparent differences in drainage travel times between Non_Frac and fractionation scenarios (Gon_Frac or CGT_Frac), but the differences between CG_Frac and CGT_Frac were noticeable almost only for precipitation events occurred during April to August of 2018 (Figure 7a) when surface soil tension remained around 10,000 cm (Figure 7b). This is because the soil texture is sandy with a steep soil water retention curve (Figure S8 in Supporting Information S1), allowing rapid recharge during high precipitation events, and draining during periods of high evaporation. Therefore, the tension effect is like an on-off process (Figure 7b) that can only be detected during dry periods.

The dynamics of RZ travel times can be divided into three stages (Figure 8d). During the early stage (between 2018/10/18–2019/03/09), the RZ (0–40 cm) water storage remained, on average, relatively high, with a mean of 2.53 cm and large fluctuations reflecting individual precipitation events (Figure 8c). The RZ travel times were relatively stable with time (2.83, 2.85, and 2.87 days on average, with a range of 0–9 days for all fractionation scenarios) (Figure 8d).

During the middle stage (between about 2019/03/10–2019/05/18), the RZ was drier (with mean water storage of 2.15 cm), increasing the root uptake stress, as discussed in Section 3.2. Therefore, the RZ travel times increased steeply with time (5.96, 5.72, and 6.04 days on average, with a range of 1–13, 0–12, and 0–13 days for the Non_Frac, CG_Frac, and CGT_Frac scenarios, respectively) compared with the early stage. This stage corresponded to April and May of 2019 when roots absorbed much more precipitation from the previous months than in other months (Figure 6b), probably due to the stimulus of increased RZ travel times during this period.

During the final stage (between 2019/05/19 and 2019/6/25), the RZ water storage increased with time (with a mean of 2.11 cm), resulting in reduced RZ travel times (5.53, 4.80, and 5.50 days on average, with a range of 0–18, 0–17, and 0–18 days for the Non_Frac, CG_Frac, and CGT_Frac scenarios, respectively).

Overall, the dynamics of drainage and RZ travel times evaluated by the virtual tracer experiment were similar to those obtained by PT. The mean drainage travel times were interpreted as 187.05, 185.18, and 185.40 days (Figures 7e–7g, Table 3), while the mean RZ travel times were interpreted as 3.93, 3.73, and 3.98 days for the Non_Frac, CG_Frac, and CGT_Frac scenarios, respectively (Figures 8e–8g, Table 3). The order of drainage and RZ travel times was in general: Non_Frac > CGT_Frac > CG_Frac. Table 3 (the last two columns) shows that the factors considered in the standard CG equation were in general more important than soil tension effects in interpreting drainage and RZ travel times.

4. Discussion

4.1. Impacts of the Soil Tension Control Versus the Standard Craig-Gordon Equation

The isotopic composition profiles (Figure 3) and the statistical indicators (Table 1) show that the results of the CG_Frac and CGT_Frac scenarios were quite similar and better than those of the Non_Frac scenario. This

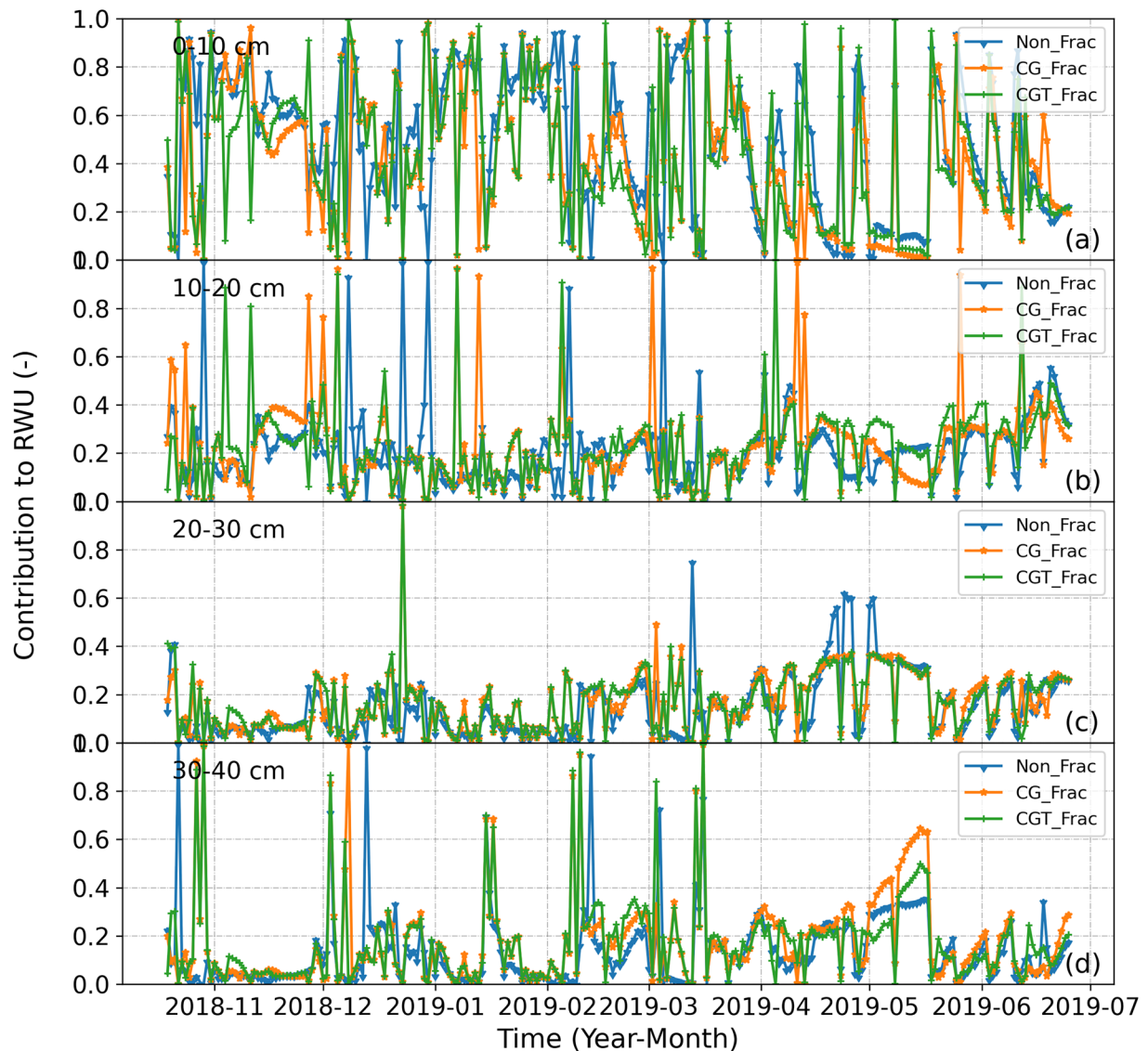


Figure 5. The contributions of different soil layers ((a) 0–10 cm, (b) 10–20 cm, (c) 20–30 cm, and (d) 30–40 cm) to root water uptake for the last 250 days of the simulation (2018/10/18–2019/06/25) interpreted by different fractionation scenarios (Non_Frac, CG_Frac, and CGT_Frac) using the SIAR model.

is because fractionation cannot be ignored in this example, as proved in the dual-isotope plot (Fig. 4 of Post et al., 2022). The soil tension control on fractionation (the CGT_Frac scenario) always resulted in a more depleted isotopic composition of soil water than the CG_Frac scenario, especially in the surface layer. This is because the total isotope flux across BCs off the model domain in the CGT_Frac is between Non_Frac and CG_Frac (Table S2 in Supporting Information S1).

For the vertical origin of RWU, considering fractionation (CG_Frac, CGT_Frac) likely resulted in a decrease in the contribution of Layer 1 and an increase in the contributions of the other soil layers (Figure 5 and Table 2). Since the isotopic compositions of surface soil water and RWU was both higher in the fractionation scenarios (CG_Frac, CGT_Frac) than in the Non_Frac scenario (Figure S4 in Supporting Information S1), a decrease in the contribution of Layer 1 may suggest that an increased isotopic composition of surface soil water exceeded that of RWU in the fractionation scenarios. The contributions of all soil layers interpreted by the CGT_Frac scenario were always between Non_Frac and CG_Frac. This is because the isotopic composition of soil water and RWU within the RZ in the CGT_Frac scenario was always between Non_Frac and CG_Frac (Figure S6 in Supporting Information S1).

Table 2
The Average Contributions of Different Soil Layers to Root Water Uptake Interpreted by Different Fractionation Scenarios (Non_Frac, CG_Frac, and CGT_Frac) Based on the Water Balance and SIAR Methods

Method	Source	Non_Frac	CG_Frac	CGT_Frac	CG_Frac relative to Non_Frac	CGT_Frac relative to CG_Frac	CGT_Frac relative to Non_Frac	Contribution of the standard CG equation (%)	Contribution of tension control (%)
WB	0–10 cm	0.603							
	10–20 cm	0.240							
	20–30 cm	0.123							
	30–40 cm	0.035							
SIAR	0–10 cm	0.493	0.426	0.444	−0.067	0.018	−0.049	79	21
	10–20 cm	0.216	0.228	0.216	0.012	−0.012	0	50	50
	20–30 cm	0.150	0.165	0.161	0.015	−0.004	0.011	79	21
	30–40 cm	0.140	0.180	0.179	0.04	−0.001	0.039	98	2

The order of drainage and RZ travel times obtained using the isotope transport-based method (VTE) was generally: Non_Frac > CGT_Frac > CG_Frac (Figures 7 and 8 and Table 3). This is because the removal of isotopes by evapotranspiration makes it difficult for isotopes to move downwards to the RZ or soil profile bottom and thus increases travel times. Since the isotope removal by evapotranspiration was largest in the Non_Frac scenario, followed by CGT_Frac and CG_Frac (Table S2 in Supporting Information S1), the travel time order was the same.

Overall, the model performance (Figure 3 and Table 1), isotope mass balance components (Table S2 in Supporting Information S1), contributions of different soil layers to RWU (Figure 5 and Table 2), and drainage and RZ travel times (Figures 7 and 8, Table 3) interpreted by the CG_Frac and CGT_Frac scenarios were much more similar than in any combination of two other scenarios (i.e., Non_Frac and CG_Frac, Non_Frac and CGT_Frac). This validates that the factors considered in the standard CG equation prevail over the soil tension control in isotope transport modeling.

4.2. Comparison of the Water Flow and Isotope Transport-Based Methods

Regarding the vertical origin, all methods reflected similar variation trends with time and depth in contributions of different soil layers to RWU. However, absolute differences always existed among different methods. The mean contributions of the middle layers (Layers 2 and 3) were similar using both methods, while those of the shallow and deep layers (Layers 1 and 4) were quite different (Table 2). This is because the SIAR model used the simulated isotopic compositions of RWU and soil water as input, and considering different fractionation scenarios resulted in considerable changes in surface isotopic compositions (Figure 3 and S6 in Supporting Information S1). On the other hand, the isotopic compositions of water sources were assumed to be arithmetic averages within the corresponding soil layers, which may not approximate reality. In addition, the vertical origin of RWU can be reliably identified only when the isotopic composition profile gradient in the RZ is large and monotonic (Allen & Kirchner, 2022; Couvreur et al., 2020). However, the “monotonic” characteristic of the RZ (0–40 cm) isotopic composition was clearly not fulfilled at least in the Non_Frac and CGT_Frac scenarios (Figure 3). This indicates that the appropriate model setup plays a vital role in ensuring the accurate identification of the vertical water origin when using the isotope transport-based methods.

Compared with the traditional in-situ isotopic measurements, the isotopic compositions of soil water and RWU in this study were obtained directly from the model output, alleviating the measurement burden and achieving higher vertical-temporal resolution (Stumpp et al., 2018). This is useful since several factors often compromise the isotopic measurements, especially under arid conditions, such as sampling spatio-temporal representativeness, instrument deficiencies, etc. (Beyer & Penna, 2021). On the other hand, we used directly the isotope composition of RWU instead of xylem water. This can avoid the uncertainty of isotopic composition changes during the water movement from the roots to the xylem (Allen & Kirchner, 2022; Barbeta et al., 2020; Chen et al., 2020).

Regarding the temporal origin, all methods revealed similar variation trends with time and relative differences between the drainage and RZ travel times interpreted by different fractionation scenarios. However, absolute

Table 3
The Mean Drainage and Root Zone Travel Times (TT) Interpreted by Different Fractionation Scenarios (Non_Frac, CG_Frac, and CGT_Frac) Based on Particle Tracking (PT) and Virtual Tracer Experiment Methods

Method	Term	Non_Frac	CG_Frac	CGT_Frac	CG_Frac relative to Non_Frac	CGT_Frac relative to CG_Frac	CGT_Frac relative to Non_Frac	Contribution of the standard CG equation (%)	Contribution of tension control (%)
PT	Drainage TT	230.96							
	RZ TT	12.64							
VTE	Drainage TT	187.05	185.18	185.40	-1.87	0.22	-1.65	89	11
	RZ TT	3.93	3.73	3.98	-0.20	0.25	0.05	44	56

disturb the isotope mass balance between upward evapotranspiration, downward infiltration, and dispersion in the RZ. This further resulted in the larger RZ travel times estimation errors by the virtual tracer experiment (relying on the isotope mass balance).

In all, the influencing factors and applicable conditions (and corresponding model inputs) of isotope transport-based methods (SIAR, virtual tracer experiment) are more complex and demanding than those considered in water flow-based (water balance, PT) methods. However, both are based (at least in this study) on numerical modeling results characterized by the equifinality problem (Beven, 2006). Therefore, it is hard to assess which approach is better. On the one hand, the simultaneous use of water flow and isotope transport-based methods may be an excellent way to provide mutual validation. On the other hand, the accuracy of these two methods should be verified by other benchmark methods, such as direct water balance measurements, artificial labeling tracers (Benettin et al., 2019; Seeger & Weiler, 2021), or tracer-based water balance analyses (Benettin et al., 2021).

4.3. Model Limitations and Future Work

Three isotope-enabled transport models are available in HYDRUS-1D: (a) the original one (Stumpp et al., 2012) is suitable when fractionation is negligible; (b) the module introduced by Zhou et al. (2021) considers the soil temperature effect on equilibrium fractionation; (c) the new module presented in this study also considers the soil tension effect on equilibrium fractionation. The soil tension effect on equilibrium fractionation is described using empirical equations (Equations 5 and 6). Replacing them with physically based equations may be possible once identified in the future.

In this study, the surface soil tension often reached 10,000 cm (Figures 7b and 8b), the soil temperature was between -7.5 and 33.5°C, and the equilibrium fractionation factor $\alpha_{v/w}$ varied from 0.946 to 0.994 for ^2H and 1.007 to 1.016 for ^{18}O in the CGT_Frac, while from 0.899 to 0.935 for ^2H and 0.988 to 0.991 for ^{18}O in the CG_Frac (Figure S5 in Supporting Information S1). The isotopic composition of surface soil water in the CGT_Frac scenario changed by -7.8‰ (for ^2H) and -3.1‰ (for ^{18}O) compared to the CG_Frac scenario (Figure 3), while the isotope mass balance components in the CGT_Frac changed up to 52% for ^2H and 20% for ^{18}O compared to the CG_Frac (Table S2 in Supporting Information S1). This suggests that a small change in $\alpha_{v/w}$ due to soil tension may result in a considerable difference in isotopic compositions and isotope mass balance. In addition, as discussed in Section 4.1, these isotopic composition and isotope mass balance differences also propagate into the interpretations of corresponding modeling results (with the SIAR model and virtual tracer experiments), albeit only to a limited magnitude.

However, only the measured isotopic profiles on the final day of the experiment were available for this study, while the impact of soil tension on equilibrium fractionation varied during the studied period (between wet and dry periods). It would thus be beneficial to have measurements available at finer time resolutions to investigate the seasonal soil tension effects. On the other hand, the field data set in this study was collected in a humid region. Changes in isotopic compositions and subsequent modeling results interpretations depend on specific experimental conditions and need further exploration, especially for arid regions (Allen & Kirchner, 2022; Finkenbiner et al., 2022).

Additionally, kinetic fractionation may affect observed isotopic enrichment more than equilibrium fractionation especially under arid conditions. For example, we conducted Partial-Least Squared Regression analysis to

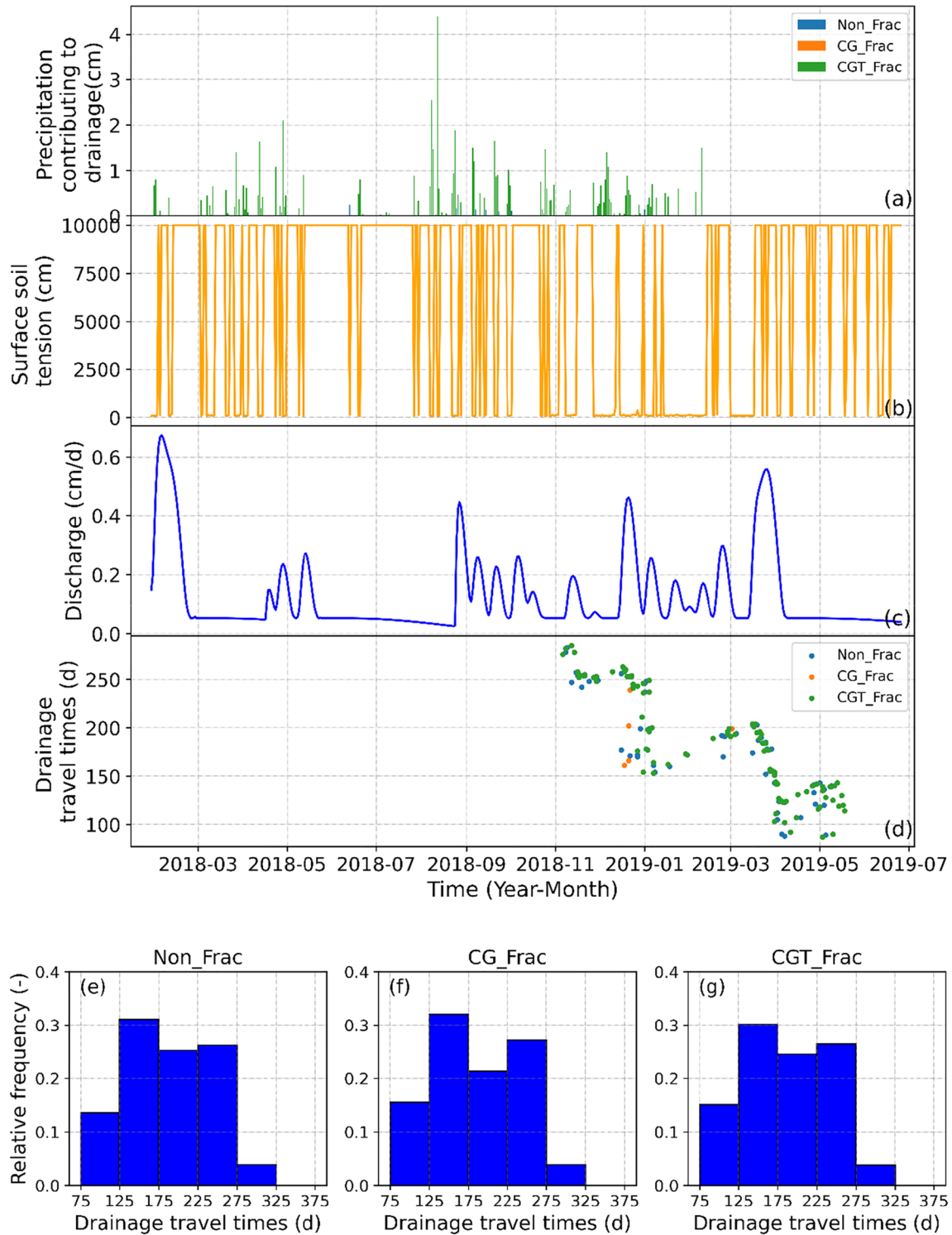


Figure 7. Precipitation (contributing to drainage) (a), surface soil tension (b), discharge (c), drainage travel times (d), and their relative frequency distributions (e–g) interpreted by different fractionation scenarios (Non_Frac, CG_Frac, and CGT_Frac) using the virtual tracer experiment.

quantify the contribution of different influencing factors of evaporation fractionation to $\delta^2\text{H}$ and $\delta^{18}\text{O}$ in the RZ (Text S6 and Table S3 in Supporting Information S1). Table S3 in Supporting Information S1 shows that the contribution of soil (or air) temperature (very close) is always greater than that of soil tension. Again, this validates that soil tension effects are much less important than temperature effects on equilibrium fractionation as

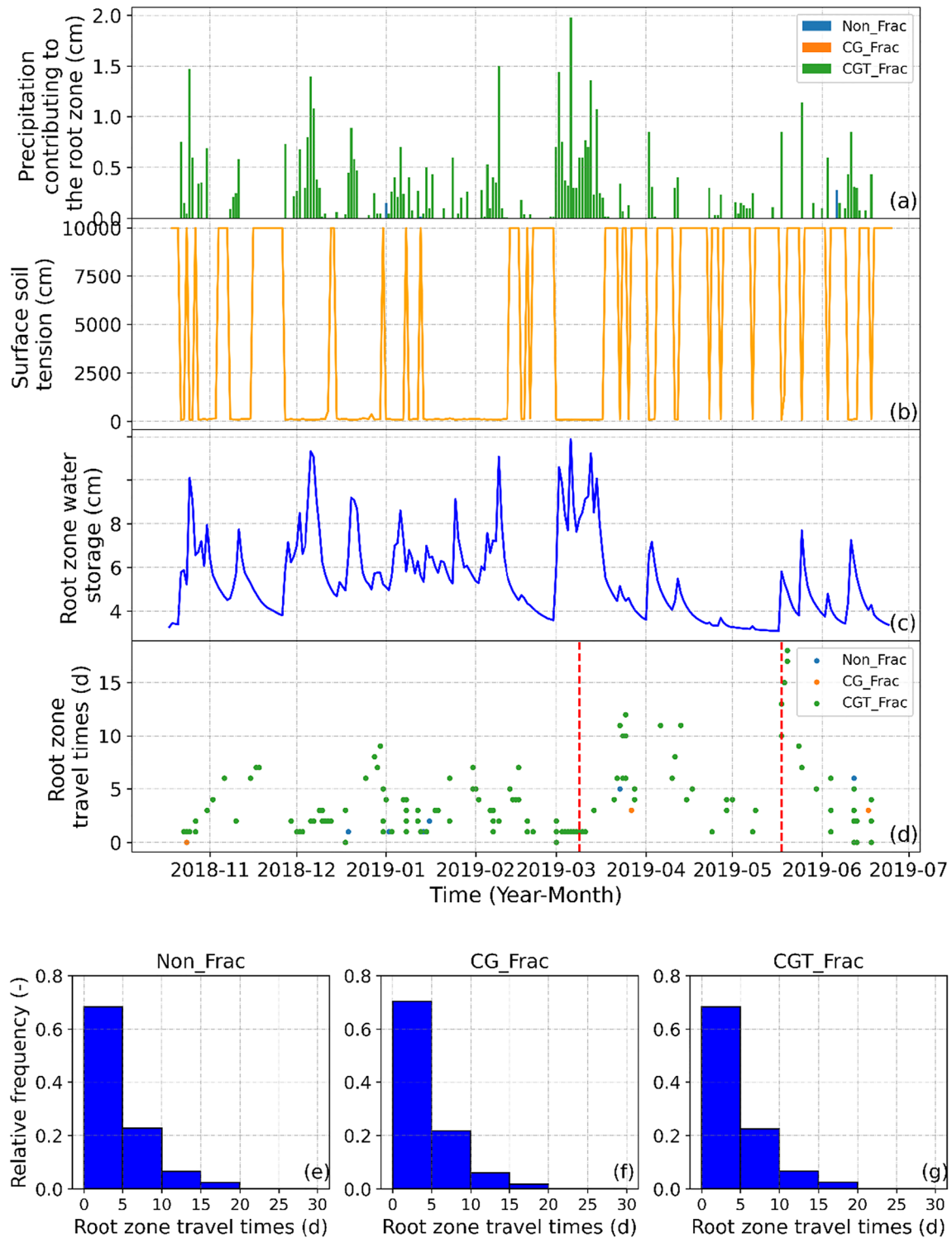


Figure 8. Precipitation (contributing to the root zone (RZ)) (a), surface soil tension (b), RZ water storage (c), RZ travel times (d), and their relative frequency distributions (e–g) interpreted by different fractionation scenarios (Non_Frac, CG_Frac, and CGT_Frac) using the virtual tracer experiment. Note that the vertical red dashed lines separate the early (between about 2018/10/18 and 2019/03/09), middle (between about 2019/03/10 and 2019/05/18), and final (between about 2019/05/19 and 2019/06/25) stages, respectively.

shown in Text S3 in Supporting Information S1. Notably, the contribution of air humidity (an indirect reflection of kinetic fractionation) is even larger than that of soil temperature for $\delta^{18}\text{O}$ (the dominant term of equilibrium fractionation). However, the impact of soil tension on kinetic fractionation is not discussed in the current literature and needs further exploration.

5. Summary and Conclusions

In this study, we first quantified the soil tension effects on evaporation fractionation and model performance in HYDRUS-1D. The results showed that additional consideration of the soil tension effect on equilibrium fractionation depletes the isotopic composition of surface soil water compared to when only the temperature effect is considered.

Regarding the vertical origin of RWU, all methods (water balance, SIAR) could reflect similar variation trends of different soil layers' contributions. The contributions of all soil layers to RWU interpreted by additionally considering soil tension effects were between the no fractionation and Craig-Gordon fractionation scenarios. The average contributions of the middle soil layers to RWU were similar using both methods, while those of the top and deep layers were quite different.

Regarding the temporal origin of RWU, all methods (PT, virtual tracer experiment) could reflect similar variation trends in drainage and RZ travel times. The order of both drainage and RZ travel times was generally: No fractionation > Craig-Gordon fractionation plus soil tension effects > Craig-Gordon fractionation. Absolute differences between different methods always existed and were more significant in RZ than drainage travel times.

Overall, considering the CG equation, rather than soil tension effects, is important for model performance, isotope mass balance, and interpreting the vertical and temporal origin of RWU. The influencing factors and applicable conditions of isotope transport-based methods (SIAR, virtual tracer experiment) are more complex and demanding than water flow-based methods (water balance, PT).

This study emphasizes the necessity of selecting a suitable model setup and simultaneously employing the water flow and isotope transport-based methods to secure reliable isotopic data interpretation. This study sheds light on future experimental designs regarding the practical applications of isotope transport modeling. However, the impacts of soil tension on isotope transport and corresponding practical applications should be further explored under arid conditions where soil tension is higher, and thus the impact of soil tension is expected to be more important.

Data Availability Statement

The software and data set used to produce the results of this study are available at Zhou, 2022 (<https://doi.org/10.5281/zenodo.7336212>).

References

- Allen, S. T., & Kirchner, J. W. (2022). Potential effects of cryogenic extraction biases on plant water source partitioning inferred from xylem-water isotope ratios. *Hydrological Processes*, 36(2), 6. <https://doi.org/10.1002/hyp.14483>
- Allen, S. T., Kirchner, J. W., Braun, S., Siegwolf, R. T. W., & Goldsmith, G. R. (2019). Seasonal origins of soil water used by trees. *Hydrology and Earth System Sciences*, 23(2), 1199–1210. <https://doi.org/10.5194/hess-23-1199-2019>
- Asadollahi, M., Stumpp, C., Rinaldo, A., & Benettin, P. (2020). Transport and water age dynamics in soils: A comparative study of spatially integrated and spatially explicit models. *Water Resources Research*, 56(3), 17. <https://doi.org/10.1029/2019wr025539>
- Barbeta, A., Gimeno, T. E., Clave, L., Frejaville, B., Jones, S. P., Delvigne, C., et al. (2020). An explanation for the isotopic offset between soil and stem water in a temperate tree species. *New Phytologist*, 227(3), 766–779. <https://doi.org/10.1111/nph.16564>
- Barnes, C. J., & Turner, J. V. (1998). Isotopic exchange in soil water. In J. J. M. C. Kendall (Ed.), *Isotope tracers in catchment hydrology* (pp. 137–164). Elsevier.
- Benettin, P., Nehemy, M. F., Asadollahi, M., Pratt, D., Bensimon, M., McDonnell, J. J., & Rinaldo, A. (2021). Tracing and closing the water balance in a vegetated lysimeter. *Water Resources Research*, 57(4), 18. <https://doi.org/10.1029/2020wr029049>
- Benettin, P., Quelo, P., Bensimon, M., McDonnell, J. J., & Rinaldo, A. (2019). Velocities, residence times, tracer breakthroughs in a vegetated lysimeter: A multitracer experiment. *Water Resources Research*, 55(1), 21–33. <https://doi.org/10.1029/2018wr023894>
- Benettin, P., Rinaldo, A., & Botter, G. (2015). Tracking residence times in hydrological systems: Forward and backward formulations. *Hydrological Processes*, 29(25), 5203–5213. <https://doi.org/10.1002/hyp.10513>
- Beven, K. (2006). A manifesto for the equifinality thesis. *Journal of Hydrology*, 320(1–2), 18–36. <https://doi.org/10.1016/j.jhydrol.2005.07.007>
- Beyer, M., & Penna, D. (2021). On the spatio-temporal under-representation of isotopic data in ecohydrological studies. *Frontiers in Water*, 3, 9. <https://doi.org/10.3389/frwa.2021.643013>

Acknowledgments

This research was financially supported by the Multistate W4188 program funded by NIFA (Grant CA-R-ENS-5047-RR). We also acknowledge the Editor Dr. Simone Fatichi, and Dr. Matthias Beyer and two other anonymous reviewers for their constructive comments on this manuscript.

- Bowers, W. H., Mercer, J. J., Pleasants, M. S., & Williams, D. G. (2020). A combination of soil water extraction methods quantifies the isotopic mixing of waters held at separate tensions in soil. *Hydrology and Earth System Sciences*, 24(8), 4045–4060. <https://doi.org/10.5194/hess-24-4045-2020>
- Brinkmann, N., Seeger, S., Weiler, M., Buchmann, N., Eugster, W., & Kahmen, A. (2018). Employing stable isotopes to determine the residence times of soil water and the temporal origin of water taken up by *Fagus sylvatica* and *Picea abies* in a temperate forest. *New Phytologist*, 219(4), 1300–1313. <https://doi.org/10.1111/nph.15255>
- Cao, M. X., Hu, A. Y., Gad, M., Adyari, B., Qin, D., Zhang, L. P., et al. (2022). Domestic wastewater causes nitrate pollution in an agricultural watershed, China. *Science of the Total Environment*, 823, 11. <https://doi.org/10.1016/j.scitotenv.2022.153680>
- Chen, Y. L., Helliker, B. R., Tang, X. H., Li, F., Zhou, Y. P., & Song, X. (2020). Stem water cryogenic extraction biases estimation in deuterium isotope composition of plant source water. *Proceedings of the National Academy of Sciences of the United States of America*, 117(52), 33345–33350. <https://doi.org/10.1073/pnas.2014422117>
- Couvreur, V., Rothfuss, Y., Meunier, F., Bariac, T., Biron, P., Durand, J. L., et al. (2020). Disentangling temporal and population variability in plant root water uptake from stable isotopic analysis: When rooting depth matters in labeling studies. *Hydrology and Earth System Sciences*, 24(6), 3057–3075. <https://doi.org/10.5194/hess-24-3057-2020>
- Craig, H. (1961). Isotopic variations in meteoric waters. *Science*, 133(346), 1702–1703. <https://doi.org/10.1126/science.133.3465.1702>
- Craig, H., & Gordon, L. (1965). Deuterium and oxygen 18 variations in the ocean and the marine atmosphere. In *Stable Isotopes in Oceanographic Studies and Paleotemperatures E, Proceedings of the Third Spoleto Conference, Spoleto, Italy* (pp. 9–130).
- Dawson, T. E., & Ehleringer, J. R. (1991). Streamside trees that do not use stream water. *Nature*, 350(6316), 335–337. <https://doi.org/10.1038/350335a0>
- Feddes, R., Kowalik, P., & Zaradny, H. (1978). *Simulation of field water use and crop yield, Simulation Monogr.* Centre for Agricultural Publishing and Documentation.
- Finkenbiner, C. E., Good, S. P., Renée Brooks, J., Allen, S. T., & Sasidharan, S. (2022). The extent to which soil hydraulics can explain ecohydrological separation. *Nature Communications*, 13(1), 1–8. <https://doi.org/10.1038/s41467-022-34215-7>
- Gaj, M., & McDonnell, J. J. (2019). Possible soil tension controls on the isotopic equilibrium fractionation factor for evaporation from soil. *Hydrological Processes*, 33(11), 1629–1634. <https://doi.org/10.1002/hyp.13418>
- Harman, C. J. (2015). Time-variable transit time distributions and transport: Theory and application to storage-dependent transport of chloride in a watershed. *Water Resources Research*, 51(1), 1–30. <https://doi.org/10.1002/2014wr015707>
- Houben, G. J., Koeniger, P., & Sultenfuss, J. (2014). Freshwater lenses as archive of climate, groundwater recharge, and hydrochemical evolution: Insights from depth-specific water isotope analysis and age determination on the island of Langeoog, Germany. *Water Resources Research*, 50(10), 8227–8239. <https://doi.org/10.1002/2014wr015584>
- Kim, M., & Harman, C. J. (2022). Transit times and StorAge selection functions in idealized hillslopes with steady infiltration. *Water Resources Research*, 58(5), 33. <https://doi.org/10.1029/2019wr025917>
- Lin, Y., & Horita, J. (2016). An experimental study on isotope fractionation in a mesoporous silica-water system with implications for vadose-zone hydrology. *Geochimica et Cosmochimica Acta*, 184, 257–271. <https://doi.org/10.1016/j.gca.2016.04.029>
- Lin, Y., Horita, J., & Abe, O. (2018). Adsorption isotope effects of water on mesoporous silica and alumina with implications for the land-vegetation-atmosphere system. *Geochimica et Cosmochimica Acta*, 223, 520–536. <https://doi.org/10.1016/j.gca.2017.12.021>
- Lipovetsky, T., Zhuang, L. W., Teixeira, W. G., Boyd, A., Pontedeiro, E. M., Moriconi, L., et al. (2020). HYPROP measurements of the unsaturated hydraulic properties of a carbonate rock sample. *Journal of Hydrology*, 591, 7. <https://doi.org/10.1016/j.jhydrol.2020.125706>
- Luo, Z., Nie, Y., Chen, H., Guan, H., Zhang, X., & Wang, K. (2023). Water age dynamics in plant transpiration: The effects of climate patterns and rooting depth. *Water Resources Research*, 59(4), e2022WR033566. <https://doi.org/10.1029/2022wr033566>
- Majoube, M. (1971). Oxygen-18 and deuterium fractionation between water and steam. *Journal of Chemical Physics*, 68(10), 1423–1436. <https://doi.org/10.1051/jcp/1971681423>
- Maloszewski, P., Maciejewski, S., Stumpp, C., Stichler, W., Trimborn, P., & Klotz, D. (2006). Modelling of water flow through typical Bavarian soils: 2. Environmental deuterium transport. *Hydrological Sciences Journal*, 51(2), 298–313. <https://doi.org/10.1623/hysj.51.2.298>
- Miguez-Macho, G., & Fan, Y. (2021). Spatiotemporal origin of soil water taken up by vegetation. *Nature*, 598(7882), 624–628. <https://doi.org/10.1038/s41586-021-03958-6>
- Nasta, P., Bonanomi, G., Šimůnek, J., & Romano, N. (2021). Assessing the nitrate vulnerability of shallow aquifers under Mediterranean climate conditions. *Agricultural Water Management*, 258, 12. <https://doi.org/10.1016/j.agwat.2021.107208>
- Orlowski, N., & Breuer, L. (2020). Sampling soil water along the pF curve for delta H-2 and delta O-18 analysis. *Hydrological Processes*, 34(25), 4959–4972. <https://doi.org/10.1002/hyp.13916>
- Pangle, L. A., Kim, M., Cardoso, C., Lora, M., Neto, A. A. M., Volkman, T. H. M., et al. (2017). The mechanistic basis for storage-dependent age distributions of water discharged from an experimental hillslope. *Water Resources Research*, 53(4), 2733–2754. <https://doi.org/10.1002/2016wr019901>
- Parnell, A. C., Inger, R., Bearhop, S., & Jackson, A. L. (2010). Source partitioning using stable isotopes: Coping with too much variation. *PLoS One*, 5(3), 5. <https://doi.org/10.1371/journal.pone.0009672>
- Post, V. E. A., & Houben, G. J. (2017). Density-driven vertical transport of saltwater through the freshwater lens on the island of Baltrum (Germany) following the 1962 storm flood. *Journal of Hydrology*, 551, 689–702. <https://doi.org/10.1016/j.jhydrol.2017.02.007>
- Post, V. E. A., Zhou, T., Neukum, C., Koeniger, P., Houben, G. J., Lamparter, A., & Šimůnek, J. (2022). Estimation of groundwater recharge rates using soil-water isotope profiles: A case study of two contrasting dune types on Langeoog Island, Germany. *Hydrogeology Journal*, 30(3), 797–812. <https://doi.org/10.1007/s10040-022-02471-y>
- Rinaldo, A., Benettin, P., Harman, C. J., Hrachowitz, M., McGuire, K. J., van der Velde, Y., et al. (2015). Storage selection functions: A coherent framework for quantifying how catchments store and release water and solutes. *Water Resources Research*, 51(6), 4840–4847. <https://doi.org/10.1002/2015wr017273>
- Seeger, S., & Weiler, M. (2021). Temporal dynamics of tree xylem water isotopes: In situ monitoring and modeling. *Biogeosciences*, 18(15), 4603–4627. <https://doi.org/10.5194/bg-18-4603-2021>
- Šimůnek, J. (1991). Numerical simulation of the transport processes in soil (in Czech, English abstract). *Vodohosp. Čas*, 39(1), 20–34.
- Sprenger, M., Seeger, S., Blume, T., & Weiler, M. (2016). Travel times in the vadose zone: Variability in space and time. *Water Resources Research*, 52(8), 5727–5754. <https://doi.org/10.1002/2015wr018077>
- Sprenger, M., Stumpp, C., Weiler, M., Aeschbach, W., Allen, S. T., Benettin, P., et al. (2019). The demographics of water: A review of water ages in the critical zone. *Reviews of Geophysics*, 57(3), 800–834. <https://doi.org/10.1029/2018rg000633>
- Stock, B. C., Jackson, A. L., Ward, E. J., Parnell, A. C., Phillips, D. L., & Semmens, B. X. (2018). Analyzing mixing systems using a new generation of Bayesian tracer mixing models. *PeerJ*, 6, 27. <https://doi.org/10.7717/peerj.5096>

- Stumpp, C., Bruggemann, N., & Wingate, L. (2018). Stable isotope approaches in vadose zone research. *Vadose Zone Journal*, *17*(1), 1–7. <https://doi.org/10.2136/vzj2018.05.0096>
- Stumpp, C., & Maloszewski, P. (2010). Quantification of preferential flow and flow heterogeneities in an unsaturated soil planted with different crops using the environmental isotope delta O-18. *Journal of Hydrology*, *394*(3–4), 407–415. <https://doi.org/10.1016/j.jhydrol.2010.09.014>
- Stumpp, C., Stichler, W., Kandolf, M., & Šimůnek, J. (2012). Effects of land cover and fertilization method on water flow and solute transport in five lysimeters: A long-term study using stable water isotopes. *Vadose Zone Journal*, *11*(1), 14. <https://doi.org/10.2136/vzj2011.0075>
- Tetzlaff, D., Birkel, C., Dick, J., Geris, J., & Soulsby, C. (2014). Storage dynamics in hydrogeological units control hillslope connectivity, runoff generation, and the evolution of catchment transit time distributions. *Water Resources Research*, *50*(2), 969–985. <https://doi.org/10.1002/2013wr014147>
- Tetzlaff, D., Piovano, T., Ala-Aho, P., Smith, A., Carey, S. K., Marsh, P., et al. (2018). Using stable isotopes to estimate travel times in a data-sparse Arctic catchment: Challenges and possible solutions. *Hydrological Processes*, *32*(12), 1936–1952. <https://doi.org/10.1002/hyp.13146>
- Timbe, E., Windhorst, D., Crespo, P., Frede, H. G., Feyen, J., & Breuer, L. (2014). Understanding uncertainties when inferring mean transit times of water trough tracer-based lumped-parameter models in Andean tropical montane cloud forest catchments. *Hydrology and Earth System Sciences*, *18*(4), 1503–1523. <https://doi.org/10.5194/hess-18-1503-2014>
- Wang, J., Lu, N., & Fu, B. J. (2019). Inter-comparison of stable isotope mixing models for determining plant water source partitioning. *Science of the Total Environment*, *666*, 685–693. <https://doi.org/10.1016/j.scitotenv.2019.02.262>
- Zhang, Y. Y., Wu, S. X., Kang, W. R., & Tian, Z. H. (2022). Multiple sources characteristics of root water uptake of crop under oasis farmlands in hyper-arid regions. *Agricultural Water Management*, *271*, 8. <https://doi.org/10.1016/j.agwat.2022.107814>
- Zhou, T. (2022). The impact of soil tension on isotope fractionation, transport, and interpretations of the root water uptake origin [Dataset]. Zenodo. <https://doi.org/10.5281/zenodo.7336212>
- Zhou, T., Šimůnek, J., & Braud, I. (2021). Adapting HYDRUS-1D to simulate the transport of soil water isotopes with evaporation fractionation. *Environmental Modelling & Software*, *143*, 105118. <https://doi.org/10.1016/j.envsoft.2021.105118>
- Zhou, T., Šimůnek, J., Braud, I., Nasta, P., Brunetti, G., & Liu, Y. (2022). The impact of evaporation fractionation on the inverse estimation of soil hydraulic and isotope transport parameters. *Journal of Hydrology*, *612*, 128100. <https://doi.org/10.1016/j.jhydrol.2022.128100>

References From the Supporting Information

- Abdi, H. (2010). Partial least squares regression and projection on latent structure regression (PLS Regression). *Wiley Interdisciplinary Reviews: Computational Statistics*, *2*(1), 97–106. <https://doi.org/10.1002/wics.51>